



Sub-150 fs dispersion-managed soliton generation from an all-fiber Tm-doped laser with BP-SA

QIAN ZHANG,¹ XINXIN JIN,¹ GUOHUA HU,^{2,3} MENG ZHANG,^{1,*}
ZHENG ZHENG,^{1,4}  AND TAWFIQUE HASAN² 

¹School of Electronic and Information Engineering, Beihang University, Beijing, 100191, China

²Cambridge Graphene Centre, University of Cambridge, Cambridge, CB3 0FA, UK

³Department of Electronic Engineering, The Chinese University of Hong Kong, Shatin, Hong Kong

⁴Beijing Advanced Innovation Center for Big Data-based Precision Medicine, Beihang University, Beijing, 100083, China

*mengzhang10@buaa.edu.cn

Abstract: We demonstrate an all-fiber, thulium-doped, mode-locked laser using a black phosphorus (BP) saturable absorber (SA). The BP-SA, exhibiting strong nonlinear response, is fabricated by inkjet printing. The oscillator generates self-starting 139 fs dispersion-managed soliton pulses centered at 1859 nm with 55.6 nm spectral bandwidth. This is the shortest pulse duration and widest spectral bandwidth achieved directly from an all-fiber thulium-doped fiber laser mode-locked with a nanomaterial saturable absorber to date. Our findings demonstrate the applicability of BP for femtosecond pulse generation at 2 μ m spectral region.

© 2020 Optical Society of America under the terms of the [OSA Open Access Publishing Agreement](#)

1. Introduction

Ultrafast fiber lasers operating at ~ 2 μ m spectral region are in demand for many applications, such as optical communications [1], gas sensing [2], mid-infrared pump sources for wavelength extension [3], and biomedical treatment [4]. Of the rare-earth doped fiber gain media, thulium (Tm)- and holmium (Ho)-doped fiber lasers have emissions at ~ 2 μ m. These fiber lasers have gained popularity due to their commercial availability for ultrashort pulse generation with versatile pulse parameters [5,6]. Given that the silica fiber shows a negative dispersion at wavelength around ~ 2 μ m, a large majority of the current Tm-doped fiber lasers operate in the soliton mode-locking regime, limiting the achievable pulse duration (sub-picosecond) and spectral bandwidth (< 10 nm) [7,8]. While obtaining ~ 150 fs soliton pulses is possible through external amplification and compression process, it is challenging to achieve such ultrashort pulses directly from a soliton laser. This is because the pulse duration (τ) of a stable fundamental soliton is limited by $\tau > \sqrt{|\beta_2|L}$, where β_2 is the group velocity dispersion (GVD), and L is the cavity length [9]. With a typical GVD of -61 ps²/km at 1.86 μ m, generation of 150 fs pulse would require 37 cm long cavity, which creates practical difficulties in compensating the dispersion and nonlinearity. An effective and compact solution to overcome this limitation is to utilize a dispersion management approach, balancing the dispersion and nonlinearity in the cavity [10–12] to achieve a close-to-zero net dispersion. In this strategy, inclusion of segments of normally and anomalously dispersive fiber allows the pulse in this cavity to experience periodic broadening and compression in each round trip. Some recent progresses have been made on dispersion-managed Tm-doped laser, with 98 fs pulse generation in a nonlinear polarization evolution (NPE) cavity [13], and 65 fs pulse generation utilizing an external chirped pulse amplification (CPA) process [14]. However, these systems are not without limitations, and usually suffer from non-fiber integration issues, environmental sensitivity, and complex configuration requirements.

For the generation of pulsed laser emission, saturable absorbers (SA) are commonly integrated into fiber lasers to provide an intensity-dependent absorption. While many SA devices have been studied for pulse generation in fiber lasers, two-dimensional (2D) nanomaterials have dominated as promising SA candidates in the past 10 years as they are easy to integrate in all-fiber systems, and exhibit wideband saturable absorption and ultrafast carrier dynamics. A number of 2D material-based SA devices (e.g. graphene [15–17], semiconducting transition metal dichalcogenides (s-TMDs) [18,19] and black phosphorus (BP) [20,21]), with parameters optimized for the use in fiber lasers operating at $\sim 2\ \mu\text{m}$, have been extensively investigated to achieve reliable mode-locking performance. The first experimental demonstration of 2D material SAs for mode-locking at $\sim 2\ \mu\text{m}$ was performed by Zhang et al. using a graphene SA to produce pulses with a duration of 3.6 ps [15]. This was followed by a growing number of studies reporting the performances of Tm-doped and Ho-doped fiber lasers mode-locked by 2D material SAs, with pulse durations covering from 0.19–1.16 ps [7,16,17,19,20,22–24], summarized in Fig. 1. The shortest pulse achieved at $\sim 2\ \mu\text{m}$ region to date is 190 fs, operating at 2060 nm with 53.6 nm bandwidth [16]. It is directly from an all-fiber, dispersion-managed Ho-doped fiber laser mode-locked with a graphene SA. Recently, BP has attracted interest as a SA material compared with zero-bandgap graphene and large bandgap TMDs. The layer-dependent band structure of BP covers from 0.3 eV (bulk) to 2 eV (monolayer), exhibiting strong photon absorption in the $2\ \mu\text{m}$ region than graphene and TMDs, making it suitable as a broad bandwidth SA for mid-infrared short-pulse technology. While great progress has been made for integrating BP into fiber lasers for pulse generation with operating wavelength range from 1 to $2.8\ \mu\text{m}$ either at discrete wavelength or with broadband tunability [25–28], the shortest pulse duration demonstrated directly from a Tm-doped fiber oscillator mode-locked by BP-SA is 739 fs [20]. Achieving $<150\ \text{fs}$ pulse at $2\ \mu\text{m}$ from a BP-SA fiber laser, is yet to be achieved.

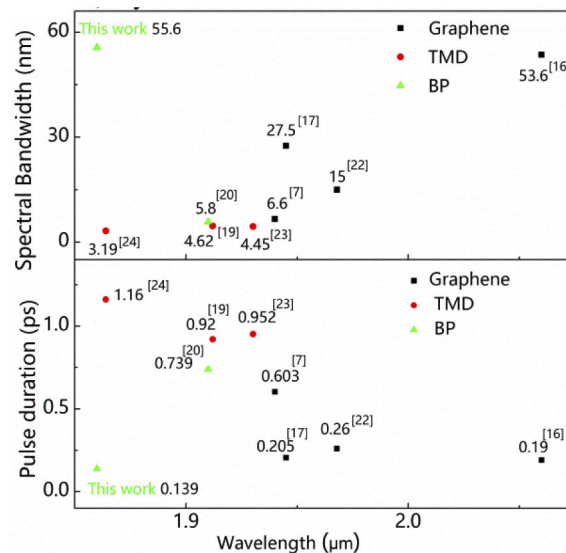


Fig. 1. Comparison of the temporal and spectral parameters of pulses from previously reported Tm-doped and Ho-doped fiber lasers mode-locked with nanomaterial SAs.

In this letter, we report an all-fiber Tm-doped laser mode-locked with an inkjet-printed BP SA. With careful control of intracavity dispersion management, the oscillator generates 139 fs pulses with 55.6 nm spectral bandwidth. This is the shortest pulse duration and widest spectral bandwidth achieved directly from an all-fiber thulium-doped fiber laser mode-locked with a nanomaterial saturable absorber reported to date. Our work demonstrates that BP has great

potential as an excellent SA at $\sim 2 \mu\text{m}$ spectral region for photonic applications requiring stable femtosecond pulses.

2. BP SA fabrication and characterization

To fabricate the SA, BP flakes ($\sim 3.4 \text{ nm}$, 6 layers) are first exfoliated from bulk crystals using ultrasound assisted liquid phase exfoliation in N-Methyl-2-pyrrolidone solvent. We then transfer the BP flakes into isopropyl alcohol through a solvent exchange process. A secondary alcohol, 2-butanol is added to formulate the BP ink. This binary solvent-based ink has a low surface tension, and low boiling points, leading to good substrate wetting and fast ink drying critical to fast ink drying, critical to avoid BP degradation [27]. The secondary alcohol used in the formulation induces a Marangoni enhanced spreading for a uniform material deposition on the substrate [29]. The printed BP thin-film on to an ultrathin ($1.5 \mu\text{m}$) polyethylene terephthalate (PET) substrate after deposition is then encapsulated with a 100 nm thick pin-hole free parylene-C passivation layer to protect it from environmental degradation [27,30]. The nonlinear saturable absorption of the fabricated BP SA is characterized using a Tm-doped fiber laser (927 fs pulse duration, 1900 nm operation wavelength, 15.4 MHz pulse repetition rate) as a pump light. The transmitted power through SA and the reference beam are recorded as a function of the incident light, while the transmitted power through the SA is recorded against a reference power. With increasing peak intensity, the transmittance of the BP SA tends to be constant, confirming saturable absorption. A typical dataset from a single measurement, at a fixed transverse position on the BP sample, can be well-fitted using a two-level SA model $T(I) = 1 - \Delta T * \exp(-I/I_{\text{sat}}) - T_{\text{ns}}$, where $T(I)$ is the intensity dependent transmission, ΔT is the modulation depth, I is the intensity of the input optical pulse, I_{sat} is the saturation power intensity, and T_{ns} is the non-saturated loss. The extracted parameters of the SA give a ΔT of 20.1% and an I_{sat} of 112 MW/cm^2 [Fig. 2] With increasing peak intensity beyond the saturation intensity (I_{sat}), the transmittance of the BP SA becomes be constant, confirming saturable absorption.

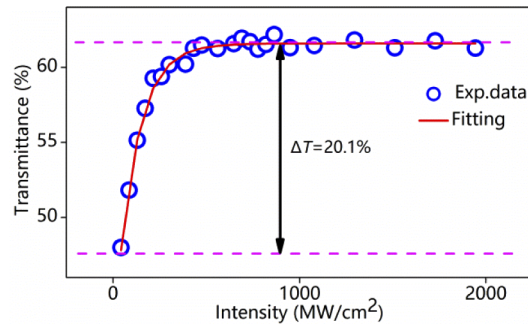


Fig. 2. Measured power-dependent transmittance of the SA at $2 \mu\text{m}$ waveband (circles, experimental data; red curve, numerical fit).

3. Experimental setup and results

We construct an all-fiber Tm-doped laser by adopting a travelling wave ring cavity configuration. The Tm-doped fiber amplifier consists of a 1.83 m -long Tm-doped active fiber (Nufern SM-TSF-9/125, with an estimated GVD of $-70 \text{ ps}^2/\text{km}$ at $1.86 \mu\text{m}$), co-pumped by a continuous-wave 1570 nm fiber laser through a 1.1 m fused $1550/1900$ wavelength division multiplexer (WDM, where its pigtail consists a piece of SMF-28e fiber with a GVD of $-61 \text{ ps}^2/\text{km}$ at $1.86 \mu\text{m}$). In addition to the fiber amplifier, the cavity comprises of an inline polarization-independent isolator to ensure unidirectional signal propagation, a 50:50 fiber output coupler for signal diagnostics, a

second WDM to extract the residual pump light and a polarization controller (PC) to adjust the intracavity birefringence. The BP-SA is inserted into a fiber laser by sandwiching it between two fiber connectors.

The performance of the laser is characterized using an optical spectrum analyzer (Yokogawa AQ6375B, with a spectral resolution of 0.05 nm), RF spectrum analyzer (Agilent N9320B, 9 kHz–3 GHz) and an oscilloscope (Agilent Technologies MSO7054A, 4 GSa/s with a photo-detector of Newport 818-BB-51F, 28 ps rising time, bandwidth > 12.5 GHz), and a commercial autocorrelator (Femtochrome FR-103XL), respectively.

When the net cavity dispersion is estimated to be -0.038 ps^2 , the laser operates in the soliton regime. The typical spectral sideband signature of deviation from average soliton operation can be observed (Fig. 4(a)). In order to shorten the pulse duration and broaden the output spectrum, 4 m long ultrahigh numerical aperture fiber (UHNA4, with an estimated GVD of $95 \text{ ps}^2/\text{km}$ at $1.86 \mu\text{m}$, calculated using the white-light interferometric technique [16,31]) is incorporated into the cavity to manage the intracavity dispersion [Fig. 3]. Figure 4 shows the evolution of the spectrum of pulses at different overall cavity group delay dispersion (GDD) when the length of the single-mode fiber (SMF) in the cavity is varied. The achievable broadest spectral bandwidth is 55.6 nm centered at 1859.3 nm, corresponding to an estimated overall cavity dispersion of 0.002 ps^2 . The entire cavity length of 9.92 m (Fig. 4(c)).

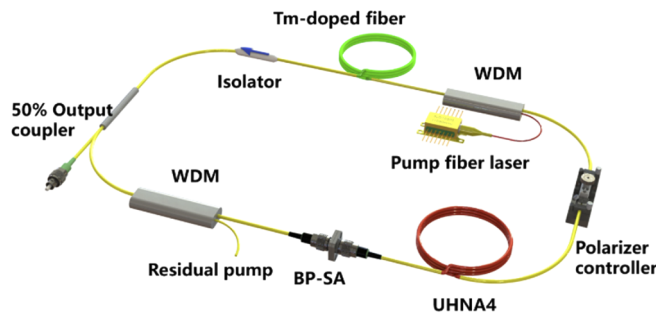


Fig. 3. Schematic diagram of the BP-SA based near zero-dispersion fiber laser.

Self-starting mode-locked performance is initiated and established by the nonlinear absorption of the BP SA at the pump power of 487 mW. Figure 5 shows the temporal and spectral diagnostics of the generated pulses at the pump power of 850 mW. A stable oscilloscope trace is observed at the fundamental repetition frequency of 20.95 MHz, with a corresponding time interval of 47.4 ns [Fig. 5(a)]. The average output power is 20.4 mW, corresponding to a single pulse energy of 0.97 nJ and peak power of 7.49 kW. The optical spectrum has a full width at half maximum (FWHM) bandwidth of 55.6 nm, and is centered at 1859.3 nm. The operating wavelength of the oscillator is affected by the gain and loss profile of the cavity. The wavelength could be moved towards the longer wavelength region by scaling the net gain of the cavity. The spikes shown on the spectrum in Fig. 5(b) are attributed to the water molecular absorption lines, with a range of 1810–1950 nm. Figure 5(c) shows the fundamental frequency spectrum of the laser output, with a signal-to-background contrast of >60 dB, indicating good mode-locking performance of the cavity. The duration of output pulses is 139 fs with an optimal length of 1.12 m of fiber pigtail of OC (Fig. 5(d)). We note that the output is fitted by a Gaussian profile. The output power of the fiber laser does not satisfy the requirement of the input power of 1-fs integration time of the autocorrelator. The 10-fs integration time we used in the measurement leads to the asymmetry of autocorrelation trace. The time-bandwidth product is 0.67. This is likely due to the uncompensated high-order dispersion. We believe that the pulses could be further compressed using an external compression strategy.

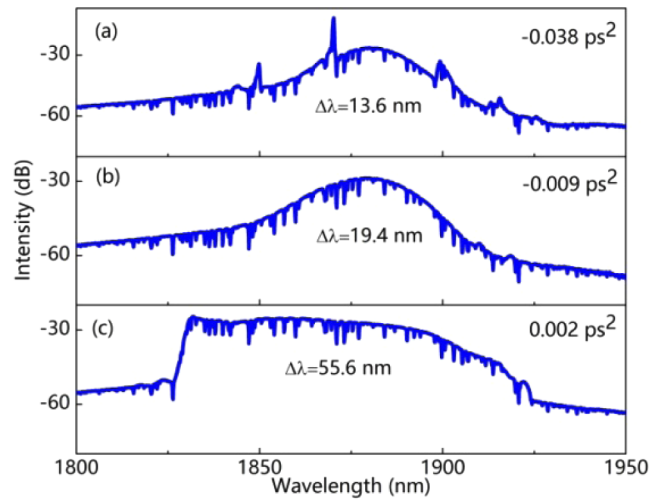


Fig. 4. output pulse spectrum when the net GDD is set at (a) -0.038 ps^2 , (b) -0.009 ps^2 , (c) 0.002 ps^2 , respectively.

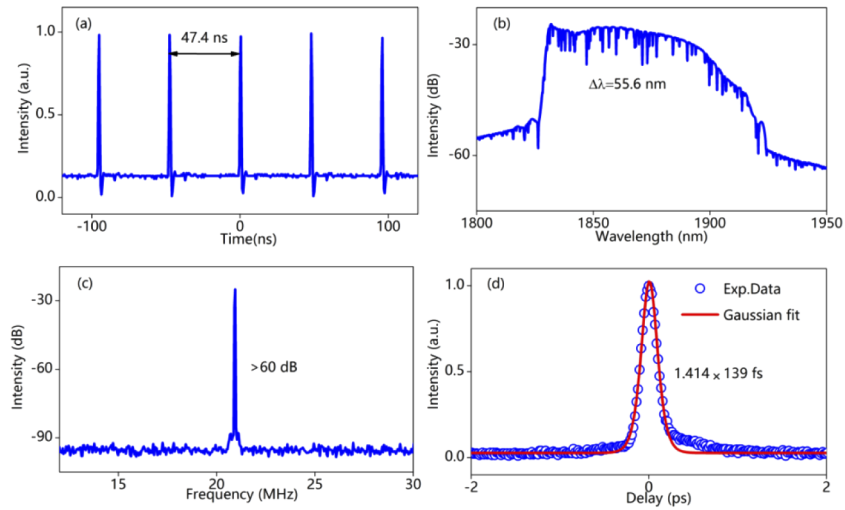


Fig. 5. Tm-doped mode-locked fiber laser: (a) Oscilloscope trace, (b) Optical spectrum, (c) Fundamental radio frequency spectrum, (d) Autocorrelation trace.

4. Conclusion

We have demonstrated an all-fiber, Tm-doped laser, mode-locked using an inkjet-printed BP-SA. The oscillator generates stable mode-locked pulses with 139 fs pulse duration and 55.6 nm spectral bandwidth. This is the shortest pulse duration and widest spectral bandwidth achieved directly from an all-fiber thulium-doped fiber laser mode-locked with a nanomaterial saturable absorber to date. The ultrafast pulse generated from our scheme can be extended to a chirped-pulse amplification system to achieve an extremely high peak power. This simple all-fiber design supporting stable operation in a small footprint represents a significant step in the ongoing development of many mid-infrared applications such as Light Detection And Ranging (LIDAR) measurements, optical free-space telecommunications, and gas sensing.

Funding

National Natural Science Foundation of China (51778030, 51978024); central public-interest Scientific Institution Basal Research Fund for Chinese Academy of Tropical Agricultural Science (No. 1630082020009).

Acknowledgments

The authors would like to acknowledge Dr. Lei Li and Junqing Zhao from Jiangsu Key Laboratory of Advanced Laser Materials and Devices for fruitful discussion.

Disclosures

The authors declare no conflicts of interest.

References

1. R. Soref, "Group IV photonics: Enabling 2 μm communications," *Nat. Photonics* **9**(6), 358–359 (2015).
2. G. D. Spiers, R. T. Menzies, J. Jacob, L. E. Christensen, M. W. Phillips, Y. Choi, and E. V. Browell, "Atmospheric CO₂ measurements with a 2 μm airborne laser absorption spectrometer employing coherent detection," *Appl. Opt.* **50**(14), 2098–2111 (2011).
3. C. R. Petersen, U. Møller, I. Kubat, B. B. Zhou, S. Dupont, J. Ramsay, T. Benson, S. Sujecki, N. Abdel-Moneim, Z. Q. Tang, D. Furniss, A. Seddon, and O. Bang, "Mid-infrared supercontinuum covering the 1.4–13.3 μm molecular fingerprint region using ultra-high NA chalcogenide step-index fibre," *Nat. Photonics* **8**(11), 830–834 (2014).
4. K. D. Polder and S. Bruce, "Treatment of Melasma Using a Novel 1,927-nm Fractional Thulium Fiber Laser: A Pilot Study," *Dermatol. Surg.* **38**(2 Part 1), 199–206 (2012).
5. J. Q. Zhao, J. Zhou, L. Li, M. Klimczak, A. Komarov, L. Su, D. Y. Tang, D. Y. Shen, and L. M. Zhao, "Narrow-bandwidth h-shaped pulse generation and evolution in a net normal dispersion thulium-doped fiber laser," *Opt. Express* **27**(21), 29770–29780 (2019).
6. M. Hinkelmann, D. Wandt, U. Morgner, J. Neumann, and D. Kracht, "Mode-locked Ho-doped laser with subsequent diode-pumped amplifier in an all-fiber design operating at 2052 nm," *Opt. Express* **25**(17), 20522–20529 (2017).
7. G. Sobon, J. Sotor, I. Pasternak, A. Krajewska, W. Strupinski, and K. M. Abramski, "All-polarization maintaining, graphene-based femtosecond Tm-doped all-fiber laser," *Opt. Express* **23**(7), 9339–9346 (2015).
8. A. Chumakovskiy, A. V. Marakulin, S. Ranta, M. Tavast, J. Rautiainen, T. Leinonen, A. S. Kurkov, and O. G. Okhotnikov, "Femtosecond mode-locked holmium fiber laser pumped by semiconductor disk laser," *Opt. Lett.* **37**(9), 1448–1450 (2012).
9. K. Tamura, E. P. Ippen, H. A. Haus, and L. E. Nelson, "77-fs pulse generation from a stretched-pulse mode-locked all-fiber ring laser," *Opt. Lett.* **18**(13), 1080 (1993).
10. L. M. Zhao, D. Y. Tang, X. Wu, D. J. Lei, and S. C. Wen, "Bound states of gain-guided solitons in a passively mode-locked fiber laser," *Opt. Lett.* **32**(21), 3191–3193 (2007).
11. F. W. Wise, A. Chong, and W. H. Renninger, "High-energy femtosecond fiber lasers based on pulse propagation at normal dispersion," *Laser Photonics Rev.* **2**(1–2), 58–73 (2008).
12. Y. Tang, A. Chong, and F. W. Wise, "Generation of 8 nJ pulses from a normal-dispersion thulium fiber laser," *Opt. Lett.* **40**(10), 2361–2364 (2015).
13. P. Li, A. Ruehl, U. Grosse-Wortmann, and I. Hartl, "Sub-100 fs passively mode-locked holmium-doped fiber oscillator operating at 2.06 μm ," *Opt. Lett.* **39**(24), 6859–6862 (2014).
14. B. Sun, J. Luo, Y. Zhang, Q. Wan, and X. Yu, "65-fs Pulses at 2 μm in a Compact Tm-Doped All-Fiber Laser by Dispersion and Nonlinearity Management," *IEEE Photon. Technol. Lett.* **30**(4), 303–306 (2018).

15. M. Zhang, E. J. R. Kelleher, F. Torrisi, Z. Sun, T. Hasan, D. Popa, F. Wang, A. C. Ferrari, S. V. Popov, and J. R. Taylor, "Tm-doped fiber laser mode-locked by graphene-polymer composite," *Opt. Express* **20**(22), 25077–25084 (2012).
16. M. Pawliszewska, T. Martynkien, A. Przewloka, and J. Sotor, "Dispersion-managed Ho-doped fiber laser mode-locked with a graphene saturable absorber," *Opt. Lett.* **43**(1), 38–41 (2018).
17. J. Sotor, J. Boguslawski, T. Martynkien, P. Mergo, A. Krajewska, A. Przewloka, W. Strupinski, and G. Sobon, "All-polarization-maintaining, stretched-pulse Tm-doped fiber laser, mode-locked by a graphene saturable absorber," *Opt. Lett.* **42**(8), 1592–1595 (2017).
18. S. Wang, H. Yu, H. Zhang, A. Wang, M. Zhao, Y. Chen, L. Mei, and J. Wang, "Broadband Few-Layer MoS₂ Saturable Absorbers," *Adv. Mater.* **26**(21), 3538–3544 (2014).
19. J. Lee, J. Koo, J. Lee, Y. M. Jhon, and J. H. Lee, "All-fiberized, femtosecond laser at 1912nm using a bulk-like MoSe₂ saturable absorber," *Opt. Mater. Express* **7**(8), 2968–2979 (2017).
20. J. Sotor, G. Sobon, M. Kowalczyk, W. Macherynski, P. Paletko, and K. M. Abramski, "Ultrafast thulium-doped fiber laser mode locked with black phosphorus," *Opt. Lett.* **40**(16), 3885–3888 (2015).
21. M. Pawliszewska, Y. Ge, Z. Li, H. Zhang, and J. Sotor, "Fundamental and harmonic mode-locking at 2.1 μm with black phosphorus saturable absorber," *Opt. Express* **25**(15), 16916–16921 (2017).
22. G. Sobon, J. Sotor, I. Pasternak, A. Krajewska, W. Strupinski, and K. M. Abramski, "260 fs and 1 nJ pulse generation from a compact, mode-locked Tm-doped fiber laser," *Opt. Express* **23**(24), 31446–31451 (2015).
23. J. Wang, H. Chen, Z. Jiang, J. Yin, J. Wang, M. Zhang, T. He, J. Li, P. Yan, and S. Ruan, "Mode-locked thulium-doped fiber laser with chemical vapor deposited molybdenum ditelluride," *Opt. Lett.* **43**(9), 1998–2001 (2018).
24. J. Wang, W. Lu, J. Li, H. Chen, Z. Jiang, J. Wang, W. Zhang, M. Zhang, I. L. Li, Z. Xu, W. Liu, and P. Yan, "Ultrafast Thulium-Doped Fiber Laser Mode Locked by Monolayer WSe₂," *IEEE J. Sel. Top. Quantum Electron.* **24**(3), 1–6 (2018).
25. M. B. Hisyam, M. F. M. Rusdi, A. A. Latiff, and S. W. Harun, "Generation of Mode-Locked Ytterbium Doped Fiber Ring Laser Using Few-Layer Black Phosphorus as a Saturable Absorber," *IEEE J. Sel. Top. Quantum Electron.* **23**(1), 39–43 (2017).
26. X. Jin, G. Hu, M. Zhang, Y. Hu, T. Albrow-Owen, R. C. T. Howe, Q. Wu, Z. Zheng, and T. Hasan, "102 fs pulse generation from a long-term stable, inkjet-printed black phosphorus-mode-locked fiber laser," *Opt. Express* **26**(10), 12506–12513 (2018).
27. G. Hu, T. Albrow-Owen, X. Jin, A. Ali, Y. Hu, R. C. T. Howe, K. Shehzad, Z. Yang, X. Zhu, R. I. Woodward, H. Jussila, P. Peng, Z. Sun, E. J. R. Kelleher, M. Zhang, Y. Xu, and T. Hasan, "Black phosphorus ink formulation for inkjet printing of optoelectronics and photonics," *Nat. Commun.* **8**(1), 278 (2017).
28. Z. Qin, G. Xie, C. Zhao, S. Wen, P. Yuan, and L. Qian, "Mid-infrared mode-locked pulse generation with multilayer black phosphorus as saturable absorber," *Opt. Lett.* **41**(1), 56–59 (2016).
29. G. Hu, L. Yang, Z. Yang, Y. Wang, X. Jin, J. Dai, Q. Wu, S. Liu, X. Zhu, X. Wang, T.-C. Wu, R. C. T. Howe, T. Albrow-Owen, L. W. T. Ng, Q. Yang, L. G. Occhipinti, R. I. Woodward, E. J. R. Kelleher, Z. Sun, X. Huang, M. Zhang, C. D. Bain, and T. Hasan, "A general ink formulation of 2D crystals for wafer-scale inkjet printing," *Sci. Adv.* **6**(33), eaba5029 (2020).
30. X. Jin, G. Hu, M. Zhang, T. Albrow-Owen, Z. Zheng, and T. Hasan, "Environmentally stable black phosphorus saturable absorber for ultrafast laser," *Nanophotonics* **9**(8), 2445–2449 (2020).
31. P. Hlubina, M. Szpulkak, D. Ciprian, T. Martynkien, and W. Urbanczyk, "Measurement of the group dispersion of the fundamental mode of holey fiber by white-light spectral interferometry," *Opt. Express* **15**(18), 11073–11081 (2007).